

High-power Characteristics of (Bi,Na)TiO₃-BaTiO₃ Ceramics and Application in Miniature Ultrasonic Motor

Susumu Miyake,^{1*} Tomohiro Harada,² Hiroyuki Shimizu,²
Sumiaki Kishimoto,² and Takeshi Morita¹

¹Graduate School of Frontier Sciences, the University of Tokyo,
5-1-5 Kashiwano-ha, Kashiwa, Chiba 277-8563, Japan

²Taiyo Yuden Co., Ltd., 5607-2 Nakamuroda, Takasaki, Gunma 370-3347, Japan

(Received February 17, 2020; accepted July 9, 2020)

Keywords: ultrasonic motor, lead-free piezoelectric material, high-power piezoelectric vibration, nonlinear vibration

Piezoelectric materials are utilized for high-power ultrasonic devices such as ultrasonic motors, which are driven under high stress and strain. The nonlinear elastic vibration of piezoelectric materials is a critical problem because it degrades the output performance. (Bi,Na)TiO₃-BaTiO₃ (BNBT) ceramics are one of the lead-free piezoelectric materials that show outstanding characteristics under high power driving, such as stable mechanical quality factor and resonance frequency. We evaluated the high-power characteristics of BNBT ceramics by measuring complex higher-order elastic constants using a nonlinear piezoelectric vibration model. We found that the absolute value of the higher-order elastic constant of BNBT was less than 4% of Pb(Zr,Ti)O₃ (PZT). Additionally, we developed a miniature ultrasonic motor using a BNBT multilayered piezoelectric transducer. This multilayered structure was utilized to enhance the piezoelectric displacement and was equipped with elastic fins, which convert the longitudinal vibration of the multilayered piezoelectric transducer into the rotational moment of the rotor. The rotational speed reached 922 rpm at a preload of 3 N under an input voltage of 58 V_{pp} and a resonance frequency of 60.0 kHz.

1. Introduction

Ultrasonic motors utilize the piezoelectric effect to convert electric input into mechanical output, which results in actuating the slider or rotor with frictional force. Recently, numerous research studies that focus on the novel design and application of ultrasonic motors have been proposed.^(1,2) However, the investigation of piezoelectric materials suitable for ultrasonic motors is limited. The characteristics of piezoelectric materials are a critical issue of ultrasonic motors because they directly affect the performance of ultrasonic motors. Pb(Zr,Ti)O₃ (PZT) is an advantageous piezoelectric material that has been applied to ultrasonic motors since its discovery.⁽³⁾ This is because of its high piezoelectric constant and outstanding temperature

*Corresponding author: e-mail: smiyake@s.h.k.u-tokyo.ac.jp
<https://doi.org/10.18494/SAM.2020.2831>

stability. However, PZT includes lead, which is harmful to human health. Therefore, various lead-free piezoelectric ceramics, such as alkaline niobate-based and barium titanate-based composite ceramics are developed as alternative materials for PZT.^(4,5) However, it is difficult to develop lead-free piezoelectric materials with both high piezoelectric properties and outstanding temperature stability similarly to PZT.⁽⁶⁾

However, some lead-free piezoelectric materials show a higher saturated vibration velocity than PZT under high electrical field, internal stress, and strain.^(7,8) In ultrasonic motors, piezoelectric transducers oscillate under high power; therefore, such excellent high-power characteristics are a promising advantage of lead-free piezoelectric materials. (Bi,Na)TiO₃-BaTiO₃ (BNBT) ceramics are one of the lead-free piezoelectric materials with such great high-power characteristics.^(9,10) In this research, we evaluated the high-power characteristics of BNBT ceramics quantitatively by evaluating complex higher-order elastic constants.⁽¹¹⁾ Admittance curves of BNBT and PZT transducers were measured and complex higher-order elastic constants were obtained by curve fitting using a nonlinear piezoelectric vibration model.^(12,13) Then, a miniature ultrasonic motor was developed using a BNBT multilayered transducer. This multilayered structure was introduced to enhance the piezoelectric displacement. The proposed stator was equipped with four elastic fins, which convert the piezoelectric linear motion into the rotational moment of the rotor.⁽¹⁴⁾

2. Evaluation of High-power Characteristics

To apply piezoelectric materials in ultrasonic motors, high-power characteristics of piezoelectric materials are a critical problem. Here, piezoelectric high-power characteristics of BNBT and PZT were evaluated quantitatively by using a nonlinear LCR equivalent circuit model.^(12,13)

2.1 Nonlinear LCR equivalent circuit method

Piezoelectric high-power characteristics can be evaluated by measuring complex higher-order elastic constants.⁽¹¹⁾ Under huge amplitude piezoelectric vibration with huge internal stress and strain, higher-order vibration is induced. It originates from the nonlinear relationship between stress and strain, which is represented as

$$T_1 = \overline{c_{11}^E} S_1 + \overline{c_{11(3)}^E} S_1^3 + \overline{e_{31}} E_3, \quad (1)$$

where T_1 , S_1 , and E_3 are the stress, strain, and electric field; $\overline{c_{11}^E}$, $\overline{c_{11(3)}^E}$, and $\overline{e_{31}}$ are the linear elastic, cubic elastic, and piezoelectric constants, respectively. Subscripts are based on the piezoelectric 31 effect because the 31 effect transducer is used to evaluate high-power characteristics in this section. The higher-order term $\overline{c_{11(3)}^E} S_1^3$ is mainly considered and other higher-order terms are omitted because the even-ordered term does not affect the signal with

driving frequency and the effect of greater than 5th-order terms is negligible compared with that of the 3rd order term.⁽¹²⁾ In this research, the cubic elastic constant $\overline{c_{11(3)}^E}$ was measured and utilized for evaluating piezoelectric high-power characteristics. $\overline{c_{11(3)}^E}$ was treated as a complex number as

$$\overline{c_{11(3)}^E} = \text{Re}\left(\overline{c_{11(3)}^E}\right) + j\text{Im}\left(\overline{c_{11(3)}^E}\right). \tag{2}$$

To obtain complex higher-order elastic constants, a nonlinear LCR equivalent circuit method is utilized.⁽⁹⁾ A general piezoelectric LCR equivalent circuit is shown in Fig. 1(a). In this circuit, the relationship between the voltage V and the current i_m is given as

$$L \frac{di_m}{dt} + Ri_m + \frac{1}{C} \int i_m dt = V, \tag{3}$$

where L , R , and C are the equivalent mass, mechanical loss, and compliance, respectively. This model is based on linear elasticity. The nonlinear LCR equivalent circuit is shown in Fig. 1(b). In this circuit, the damped capacitance C_d and force factor A are considered constant and the equivalent mechanical loss R and compliance C are functions of the current i_m . Hence, Eq. (3) is modified as

$$L \frac{di_m}{dt} + R_0 i_m + \eta i_m^3 + \frac{1}{C_0} \int i_m dt + \xi \omega^3 \left(\int i_m dt \right)^3 = V, \tag{4}$$

where ω is the angular frequency, η is the nonlinear mechanical loss coefficient, and ξ is the nonlinear compliance coefficient. The admittance $Y = i_m/V$ can be calculated using Eq. (4). In the next section, the admittance curve of BNBT and PZT plate transducers was measured and the nonlinear coefficients η and ξ were obtained by admittance curve fitting using Eq. (4).

Complex higher-order elastic constants $\overline{c_{11(3)}^E}$ were obtained on the basis of their relationship with η and ξ as

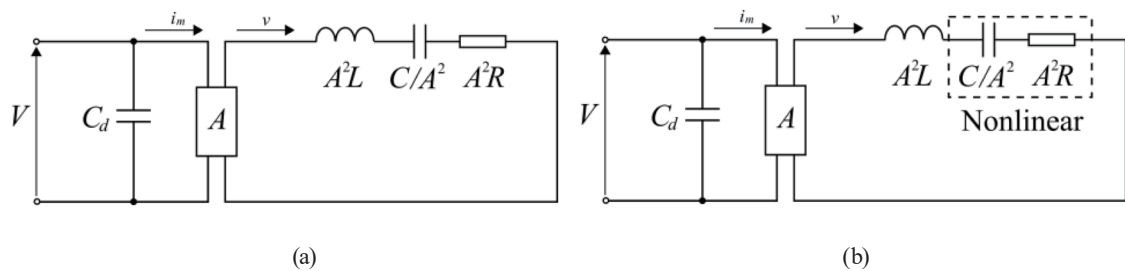


Fig. 1. (a) General LCR equivalent circuit. (b) Nonlinear LCR equivalent circuit.

$$\operatorname{Re}\left(\overline{c_{11(3)}^E}\right) = \frac{16}{9} \frac{\overline{c_{11}^E}^2 A^2}{\rho \omega_r L} \xi, \quad (5)$$

$$\operatorname{Im}\left(\overline{c_{11(3)}^E}\right) = \frac{16}{9} \frac{\overline{c_{11}^E}^2 A^2}{\rho \omega_r L} \eta, \quad (6)$$

where ρ and ω_r are the density and resonance frequency, respectively.

2.2 Admittance curve measurement

Figure 2 shows the setup of the admittance curve measurement. BNBT (Taiyo Yuden Co., Ltd., $4 \times 0.8 \times 10 \text{ mm}^3$) and PZT (Fuji Ceramics Corporation, C-203, $7 \times 2 \times 44 \text{ mm}^3$) transducers were prepared. The measured admittance curves of the BNBT and PZT transducers are shown in Figs. 3 and 4, respectively. The admittance curve of the PZT transducer showed clear admittance jumping and a 1.5% resonance frequency shift; however, the BNBT transducer

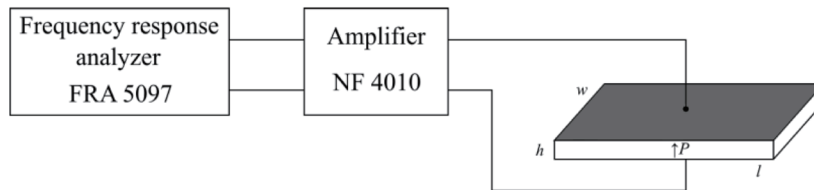


Fig. 2. Setup of admittance curve measurement.

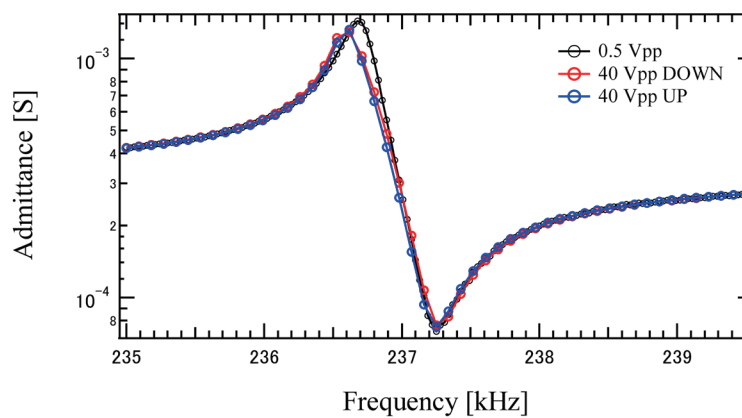


Fig. 3. (Color online) Admittance curve of BNBT transducer.

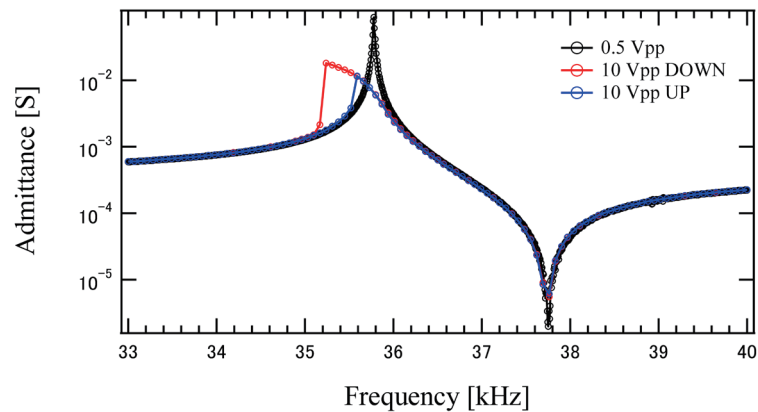


Fig. 4. (Color online) Admittance curve of PZT transducer.

showed only a 0.03% resonance frequency shift. Using Eqs. (4)–(6), we applied fitting to these admittance curves, and complex higher-order elastic constants were obtained as shown in Table 1. Higher-order elastic constants of BNBT were less than 4% of those of PZT. From Eq. (1), small higher-order elastic constants prevent higher-order vibration. Therefore, BNBT can be considered as a promising piezoelectric material that is excited under high power.

3. Ultrasonic Motor Using BNBT Multilayered Transducer

3.1 Design of ultrasonic motor

We developed a miniature ultrasonic motor using a BNBT multilayered transducer. The proposed ultrasonic motor and its rotor part are shown in Figs. 5 and 6, respectively. The dimensions of the BNBT multilayered transducer were $5 \times 5 \times 8 \text{ mm}^3$ and the transducer consists of 140 layers. On the top surface of the multilayered transducer, four L-shaped elastic fins and the shaft were bonded. These elastic fins were made of beryllium copper and the angle of the fins was 15° . When the BNBT multilayered transducer was excited by the 1st longitudinal resonance mode, these elastic fins converted the longitudinal displacement of the multilayered transducer into the rotational movement of the rotor. The preload was given by the upper spring, whose spring constant was 0.118 or 0.765 N/mm.

The driving principle of the elastic fin motor is shown in Fig. 7. From initial state (a) to state (b), the stator (BNBT multilayered transducer) moves upward and the rotor and elastic fin move together without slippage because of sufficient normal force (= preload force + force from the stator). In state (c), when the stator moves downward, the normal force (= preload – force from the stator) decreases and slippage occurs. At the end of state (c), the rotor rotates in the right direction from state (a). In this manner, the rotor can be driven in one direction by repeating the cycle of state from (a) to (c).

Table 1
Complex higher-order elastic constants of BNBT and PZT.

	$\text{Re}\left(\overline{c_{11(3)}^E}\right) (\text{N/m}^2)$	$\text{Im}\left(\overline{c_{11(3)}^E}\right) (\text{N/m}^2)$
BNBT	-1.4×10^{15}	3.2×10^{14}
PZT	-1.3×10^{17}	8.5×10^{15}

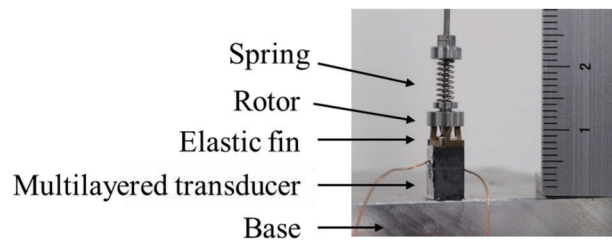


Fig. 5. (Color online) Proposed ultrasonic motor.

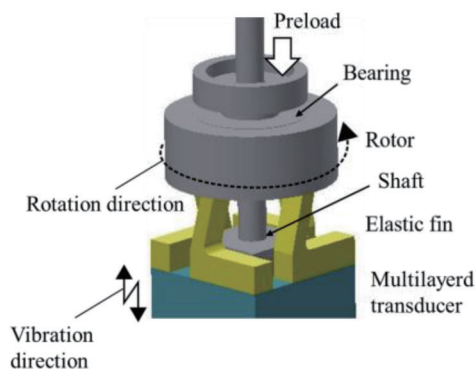


Fig. 6. (Color online) Rotor part of ultrasonic motor.

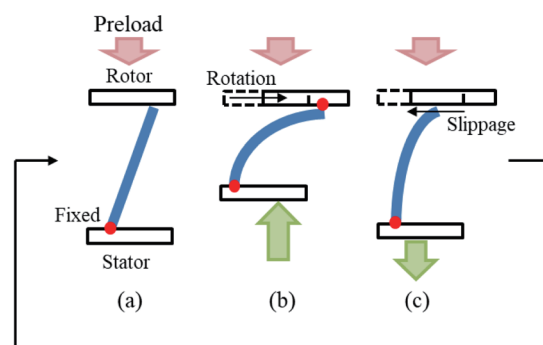


Fig. 7. (Color online) Driving principle of elastic fin motor.

3.2 Measurement

To evaluate the performance of the ultrasonic motor, the rotational speed of the rotor was measured using a laser doppler velocimeter (Cannon S-100Z). The experimental setup is shown in Fig. 8. The relationship between the rotational speed and the input voltage at preloads of 2 and 3 N is shown in Fig. 9. The motor was driven by the 1st resonance frequency, which shifted from 60.2 to 60.0 kHz when the preload was changed from 2 to 3 N. However, the resonance frequency did not change with the driving voltage amplitude. In general, resonant ultrasonic motors exhibit a resonance frequency shift depending on the driving voltage. This is caused by the nonlinear vibration of piezoelectric materials. As confirmed in Sect. 2, the outstanding high-power characteristics of BNBT result in the stability of the resonance frequency of the proposed motor. The rotational speed increased with the input voltage and finally saturated. The rotation at a preload of 3 N was unstable compared with that at a preload of 2 N and no rotation was confirmed at a preload of 4 N. This is because a very large preload inhibits

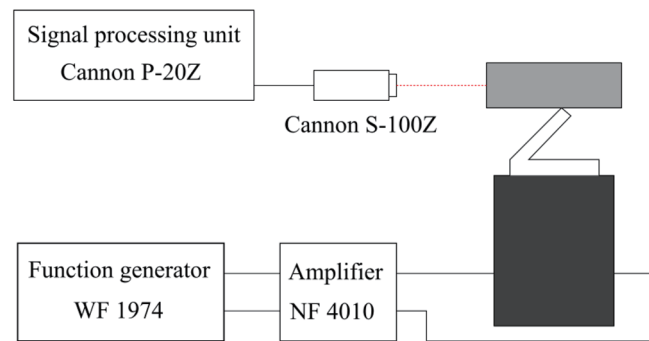


Fig. 8. (Color online) Experimental setup to measure rotational speed.

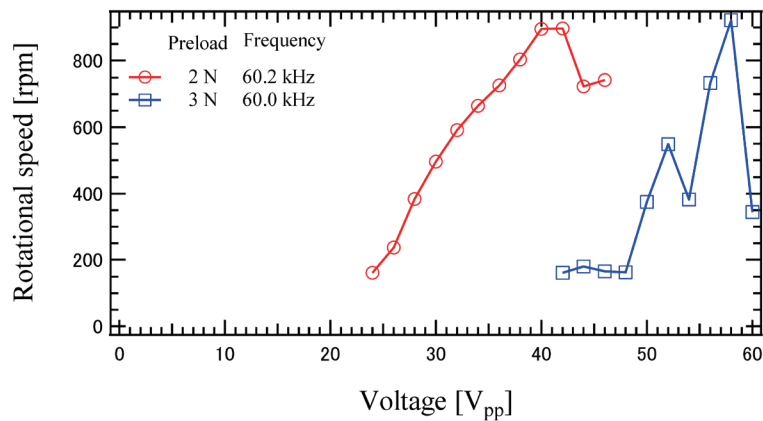


Fig. 9. (Color online) Relationship between voltage and rotational speed.

Table 2
Comparison with other miniature ultrasonic motors.

Design	Transducer size (mm)	Piezoelectric material	d_{33} (pC/N)	Rotational speed (rpm)
Zhao <i>et al.</i> ⁽¹⁵⁾	Ø11.5 × Ø7.5 × 0.45 (50 μm × 9 layers)	PZT	593	2100
Doshida <i>et al.</i> ⁽¹⁶⁾	12 × 3 × 1	(Sr,Ca) ₂ NaNbO ₁₅	260	190
Proposed motor	5 × 5 × 8	BNBT	77	922

slippage in the state in Fig. 3(c). The maximum rotational speed was determined to be 898 rpm at a preload of 2 N and 922 rpm at a preload of 3 N. Table 2 shows the performance comparison of our proposed ultrasonic motor with existing miniature ultrasonic motors that use the PZT multilayer transducer⁽¹⁵⁾ and crystal-oriented (Sr,Ca)₂NaNbO₁₅ transducer.⁽¹⁶⁾ (Sr,Ca)₂NaNbO₁₅ is a lead-free piezoelectric material with great high-power characteristics reported by Doshida *et al.*^(9,10) Our proposed ultrasonic motor showed the smallest piezoelectric constant ($d_{33} = 77$ pC/N) and a higher rotational speed than the lead-free ultrasonic motor. We have to consider that Doshida *et al.* used 31 mode piezoelectric vibration of stator transducer, but our proposed motor realized high rotational speed owing to the multilayered structure and BNBT's high-power characteristics.

4. Conclusions

In this research, complex higher-order elastic constants of BNBT ceramics were evaluated using a nonlinear LCR equivalent circuit model. The measured complex higher-order elastic constants of BNBT were less than 4% of PZT. This indicates that BNBT is a promising piezoelectric material under high power. A miniature elastic fin-type ultrasonic motor was developed utilizing a BNBT multilayered transducer. It provided stability of resonance frequency, and the maximum rotational speed reached 922 rpm at a preload of 3 N under an input voltage of 58 V_{pp}. The performance difference between BNBT and lead-based piezoelectric materials will be examined in terms of their usage for the stator of the ultrasonic motor.

Acknowledgments

This work was supported by JSPS KAKENHI Grant number JP18J22170.

References

- 1 T. Morita: *Sens. Actuators, A* **103** (2003) 291. [https://doi.org/10.1016/S0924-4247\(02\)00405-3](https://doi.org/10.1016/S0924-4247(02)00405-3)
- 2 K. Uchino: *J. Electroceram.* **20** (2008) 301. <https://doi.org/10.1007/s10832-007-9196-1>
- 3 B. Jaffe, R. S. Roth, and S. Marzullo: *J. Appl. Phys.* **25** (1954) 809. <https://doi.org/10.1063/1.1721741>
- 4 Y. Saito, H. Takao, T. Tani, T. Nonoyama, K. Takatori, T. Nomma, T. Nagaya, and M. Nakamura: *Nature* **432** (2004) 84. <https://doi.org/10.1038/nature03028>
- 5 T. Takenaka and H. Nagata: *J. Eur. Ceram. Soc.* **25** (2005) 2693. <https://doi.org/10.1016/j.jeurceramsoc.2005.03.125>
- 6 T. R. Shrout and S. J. Zhang: *J. Electroceramics* **19** (2007) 111. <https://doi.org/10.1007/s10832-007-9047-0>
- 7 Y. Himura, T. Watanabe, H. Nagata, and T. Takenaka: *Jpn. J. Appl. Phys.* **47** (2008) 7659 <https://doi.org/10.1143/JJAP.47.7659>
- 8 Y. Noumura, S. Sato, Y. Hiruma, H. Nagata, and T. Takenaka: *Trans. Mater. Res. Soc. Jpn.* **36** (2011) 363. <https://doi.org/10.14723/tmrj.36.363>
- 9 Y. Doshida, H. Shimizu, Y. Mizuno, and H. Tamura: *Jpn. J. Appl. Phys.* **52** (2013) 09ND06. <https://doi.org/10.7567/JJAP.52.07HE01>
- 10 Y. Doshida, H. Shimizu, Y. Mizuno, K. Itoh, S. Hirose, and H. Tamura: *Jpn. J. Appl. Phys.* **50** (2011) 09ND06. <https://doi.org/10.1143/JJAP.50.09ND06>
- 11 S. Miyake, T. Kasashima, M. Yamazaki, Y. Okimura, H. Nagata, H. Hosaka, and T. Morita: *Jpn. J. Appl. Phys.* **57** (2018) 07LB14. <https://doi.org/10.7567/JJAP.57.07LB14>
- 12 Y. Liu, R. Ozaki, and T. Morita: *Sens. Actuators, A* **227** (2015) 31. <https://doi.org/10.1016/j.sna.2015.03.036>
- 13 Y. Liu and T. Morita: *Jpn. J. Appl. Phys.* **54** (2015) 10ND01 <https://doi.org/10.7567/JJAP.54.10ND01>
- 14 M. Kurosawa, T. Uchiki, H. Hanada, K. Nakamura, and S. Ueha: *Proc. IEEE 1992 Ultrasonics Symp. (IEEE, 1992)* 893. <https://doi.org/10.1109/ULTSYM.1992.275843>
- 15 Y. Zhao, S. Yuan, X. Chu, S. Gao, Z. Zhong, and C. Zhu: *Rev. Sci. Instrum.* **87** (2016) 095108. <https://doi.org/10.1063/1.4963662>
- 16 Y. Doshida, H. Tamura, and S. Yanaka: *Jpn. J. Appl. Phys.* **58** (2019) SGGA07. <https://doi.org/10.7567/1347-4065/ab0bad>

About the Authors



Susumu Miyake received his B.S. Eng. and M.S. degrees from the University of Tokyo in 2016 and 2018, respectively. He is currently pursuing his doctorate degree at the University of Tokyo. His current research interests are in the high-power characteristics of piezoelectric and lead-free piezoelectric materials. (smiyake@s.h.k.u-tokyo.ac.jp)



Tomohiro Harada received his M.S. degree in engineering science from Tokyo University of Science in 2009. He has been working on piezoelectric material design and processing at Taiyo Yuden Co., Ltd., since 2009. In 2018, he received an award for an outstanding paper published in the JCS-Japan in the field of crystal orientation of piezoelectric ceramics. His current research interests are in lead-free piezoelectric materials and high-power applications. (tharada@jty.yuden.co.jp)



Hiroyuki Shimizu received his Ph.D. degree in materials science from Nara Institute of Science and Technology in 2006. He has been working on piezoelectric material design and actuator development in Taiyo Yuden Co., Ltd. since 2006. He received the 66th JCS-Japan award for advancement in industrial ceramic technology in 2012 in the field of textured ceramic design. From 2012 to 2014, he researched on antiferroelectric and piezoelectric materials as a visiting scientist in Pennsylvania State University. His current research and development focuses on lead-free piezoelectric materials and applications. (h-shimizu@jty.yuden.co.jp)



Sumiaki Kishimoto received his M.S. degree in electrical engineering from Tokyo University of Science in 2002. He has been working on process technology for MLCC and piezoelectric materials in Taiyo Yuden Co., Ltd., since 2002. Currently, he is the manager in charge of piezoelectric material development. His current research interests are in piezoelectric materials and applications in sensors and actuators. (s-kishimoto@jty.yuden.co.jp)



Takeshi Morita received his B.S. Eng., M.S. Eng., and Ph.D. Eng. degrees in precision machinery engineering from The University of Tokyo in 1994, 1996, and 1999, respectively. After working as a postdoctoral researcher at RIKEN (the Institute of Physical and Chemical Research) and EPFL (Swiss Federal Institute of Technology), he became a research associate at Tohoku University in 2002. He obtained a position at The University of Tokyo as an associate professor in 2005 and has been a full professor since 2018. His research interests include piezoelectric actuators and sensors, and their fabrication processes and control systems. (morita@edu.k.u-tokyo.ac.jp)